Physical Properties and Enzymatic Degradability of Polymer Blends of Bacterial Poly[(*R*)-3-hydroxybutyrate] and Poly[(*R*,*S*)-3-hydroxybutyrate] Stereoisomers

Hideki Abe, Isao Matsubara,† and Yoshiharu Doi*

Polymer Chemistry Laboratory, The Institute of Physical and Chemical Research (RIKEN), Hirosawa, Wako-shi, Saitama 351-01, Japan

Received August 12, 1994; Revised Manuscript Received November 9, 1994®

ABSTRACT: Three stereocopolymers of poly[(*R*,*S*)-3-hydroxybutyrate] (P[(*R*,*S*)-3HB]) containing both *R* and *S* units; atactic P[(*R*,*S*)-3HB] with 70% (*R*)-3-hydroxybutyrate ((*R*)-3HB) (ata-P[70%(*R*)-3HB]), syndiotactic P[(*R*,*S*)-3HB] with 50% (*R*)-3HB (syn-P[50%(*R*)-3HB]), and atactic P[(*R*,*S*)-3HB] with 50% (*R*)-3HB (ata-P[50%(*R*)-3HB]), were prepared by ring-opening polymerization of (*R*)- and (*S*)-β-butyrolactone in the presence of 1-ethoxy-3-chlorotetrabutyldistannoxane catalyst or diethylzinc/water (1.0/0.6) catalyst. The physical properties of binary blends of bacterial P[(*R*)-3HB] with chemosynthetic P[(*R*,*S*)-3HB] were investigated by means of DSC, optical microscopy, X-ray diffraction, and tensile test. The glass-transition temperatures of each polymer blend were 5 ± 2 °C, independently of P[(*R*,*S*)-3HB] content. The equilibrium melting temperature of binary blends decreased from 191 to 174 °C as P[(*R*,*S*)-3HB] content was increased from 0 to 75 wt %, suggesting that the P[(*R*)-3HB] and P[(*R*,*S*)-3HB] polymers are miscible in the melt and in the amorphous state. The degrees of crystallinity of P[(*R*)-3HB]/P[(*R*,*S*)-3HB] blend films decreased with an increase in the P[(*R*,*S*)-3HB] content. The enzymatic degradation of blend films were carried out in a 0.1 M potassium phosphate buffer (pH 7.4) at 37 °C in the presence of PHB depolymerase from *Pseudomonas pickettii*. The enzymatic hydrolysis of polymer chains took place on the surface of P[(*R*)-3HB] film, while little hydrolysis occurred on the surface of atactic and syndiotactic P[(*R*,*S*)-3HB] stereoisomers. However, when P[(*R*,*S*)-3HB] stereoisomers were blended with P[(*R*)-3HB], the enzymatic erosion of films were accelerated, and the highest rates of enzymatic hydrolysis were observed at around 50 wt % of P[(*R*,*S*)-3HB] content. Water-soluble products liberated during the enzymatic degradation of P[(*R*)-3HB]/P[(*R*,*S*)-3HB] blend films were characterized by HPLC analysis. Bacterial P[(*R*)-3HB] film produced a mixture of monomer and dimer of 3-hydroxybutyric acid, while P[(*R*)-3HB]/P[(*R*,*S*)-3HB] blend films gave a mixture of monomer, dimer, trimer, and tetramer, which suggests that atactic and syndiotactic P[(*R*,*S*)-3HB] components are hydrolyzed by PHB depolymerase in the presence of P[(*R*)-3HB] component. A model of enzymatic hydrolysis of P(3HB) chains by PHB depolymerase is proposed on the basis of above results.

Introduction

A wide variety of bacteria synthesize an optically active polymer of (*R*)-3-hydroxybuyric acid and accumulate it as an intracellular storage material of carbon and energy.[1,2] Poly[(*R*)-3-hydroxybutyrate] (P[(*R*)-3HB]) isolated from bacteria is a biodegradable thermoplastic with a melting temperature around 180 °C.[3,4] The bacterial P[(*R*)-3HB] has attracted industrial attention as a possible candidate of the large biotechnological products.[5]

A remarkable characteristic of P[(*R*)-3HB] is its biodegradability in the environment. P[(*R*)-3HB] films are degraded in soil, sludge, or seawater, and the degradation rate is extremely fast under optimum conditions.[1] Aerobic and anaerobic P[(*R*)-3HB]-degrading bacteria and fungi have been isolated from various environments.[6−15] The microorganisms excrete extracellular PHB depolymerases to degrade environmental P[(*R*)-3HB] and utilize the decomposed compounds as nutrients. The extracellular PHB depolymerases have been purified from some microorganisms such as *Pseudomonas lemoignei*,[16] *P. pickettii*,[13] *P. fluoresens*,[12] *P. stutzeri*,[15] *Alcaligenes faecalis*,[8] *Comamonas testosteroni*,[14] *Comamonas* sp.,[11] and *Penicillium funiculosum*.[17]

Recently, Kumagai *et al.*[18] reported that the rate of enzymatic hydrolysis of P[(*R*)-3HB] film by PHB depolymerase from *A. faecalis* was increased with a decrease in the crystallinity. In addition, stereochemical effects on the rate of enzymatic degradation have been studied using synthetic P[(*R*,*S*)-3HB] containing both *R* and *S* units. The chemical synthesis of poly(3-hydroxybutyrate) (P(3HB)) has been achieved by the ring-opening polymerization of mixture of (*R*)- and (*S*)-β-butyrolactone (β-BL) in the presence of aluminum-,[19−31] zinc-,[21,22,31−34] or tin-based[35−37] catalysts. The chemosynthetic P(3HB) is an interesting model polymer to investigate the stereochemical and morphological effects on the rate of biodegradation. Stereoblock copolymers of P(3HB), with sequences of predominantly *R* and predominantly *S* units, can be prepared by the polymerization of racemic β-BL with aluminum-based catalysts, and fractionated to yield a range of tacticities. Doi *et al.*[27] and Marchessault *et al.*[38] demonstrated that a low-crystalline atactic P(3HB) fraction was degraded more readily than more crystalline, predominantly isotactic P(3HB) fractions in the presence of PHB depolymerase from *A. faecalis*. More recently, Marchessault *et al.*[39] fractionated P(3HB) polymers into several components with a wide range of isotacticities varying from 0.35 to 0.88, and studied the stereochemical effects on the rate of enzymatic degradation with PHB depolymerases from *P. lemoignei* and *A. fumigatus*. Low crystalline P(3HB) components (55-60% isotactic diads) showed significantly higher rates of enzymatic degradation than those of more crystalline P(3HB) components

* Author to whom correspondence should be addressed.
† Current address: Tokyo Institute of Technology, Nagatsuta 4259, Midori-ku, Yokohama 227, Japan.
® Abstract published in *Advance ACS Abstracts*, January 15, 1995.

0024-9297/95/2228-0844$09.00/0

with either an isotactic or a syndiotactic crystal structure. However, the rate of enzymatic degradation on the low-crystalline, atactic P(3HB) material containing 50% (*R*) and 50% (*S*) units was lower than the rate on the bacterial P[(*R*)-3HB] material.

Zinc-based catalysts produce a stereorandom copolymer of (*R*)- and (*S*)-3HB units. Kemnitzer *et al.*[34] prepared P(3HB) stereoisomers of relatively low molecular weights ($M_n = 3.5-7.0 \times 10^3$) by the stereorandom copolymerization of (*R*)-β-BL with (*S*)-β-BL at various feed monomer ratios in the presence of $ZnEt_2/H_2O$ catalyst. The fraction of (*R*)-3HB units in P[(*R*,*S*)-3HB] was varied from 6 to 94%, and the stereochemical effects on the rate of enzymatic degradation were studied with the PHB depolymerase from *P. funiculosum*.[16] They demonstrated that the rate of enzymatic degradation of P[77%(*R*)-3HB] was several times higher than the rate of bacterial P[(*R*)-3HB], but that P[94%-(*S*)-3HB] was hardly hydrolyzed by the enzyme. In a previous paper,[40] we studied the physical properties and enzymatic degradability of P[(*R*,*S*)-3HB] stereoisomers of high molecular weights ($M_n > 10^5$) prepared by the ring-opening copolymerization of (*R*)- and (*S*)-β-BL at various feed ratios (*R*/*S* = 96/4 to 50/50) in the presence of 1-ethoxy-3-chlorotetrabutyldistannoxane as a catalyst. The isotactic diad fraction [*i*] of P(3HB) stereoisomers decreased from 0.92 to 0.30, as the fraction of (*R*)-β-BL in feed was decreased from 0.96 to 0.50. The physical and thermal properties of P[(*R*,*S*)-3HB] stereoisomers were shown to be strongly dependent of the stereoregularity. The enzymatic degradation of P[(*R*,*S*)-3HB] films with different stereoregularities depended on PHB depolymerases from *P. pickettii* and *A. faecalis*, and showed that the rates of enzymatic degradation of P[(*R*,*S*)-3HB] films ranging in the [*i*] value from 0.68 to 0.92 were higher than that of bacterial P[(*R*)-3HB] film ([*i*] = 1.00). However, the amorphous P[70%(*R*)-3HB] sample ([*i*] = 0.46) with 70% (*R*)-3HB and syndiotactic P[50%(*R*)-3HB] sample ([*i*] = 0.30) with 50% (*R*)-3HB were hardly hydrolyzed by the PHB depolymerases.

Abe *et al.*[41] studied the morphology and properties of binary blend of bacterial P[(*R*)-3HB] and atactic P[(*R*,*S*)-3HB], which was prepared by the polymerization of racemic β-BL with $ZnEt_2/H_2O$ catalyst, and showed that the atactic P[(*R*,*S*)-3HB] was miscible with P[(*R*)-3HB] in the melt and included in the amorphous regions between the lamellae of P[(*R*)-3HB] under certain crystallization conditions. Kumagai *et al.*[42] studied the enzymatic degradability of the blends of P[(*R*)-3HB] with atactic P[(*R*,*S*)-3HB] with the PHB depolymerase from *A. faecalis*. The rates of enzymatic degradation of the blend films were higher than those of the corresponding P[(*R*)-3HB] and P[(*R*,*S*)-3HB] films, and the highest rate was observed at about 50 wt% of P[(*R*,*S*)-3HB] component.

In this paper, we prepare three samples of P[(*R*,*S*)-3HB]: atactic P[(*R*,*S*)-3HB] ([*i*] = 0.46) with 70% (*R*)-3HB (ata-P[70%(*R*)-3HB]), syndiotactic P[(*R*,*S*)-3HB] ([*i*] = 0.30) with 50% (*R*)-3HB (syn-P[50%(*R*)-3HB]), and atactic P[(*R*,*S*)-3HB] ([*i*] = 0.51) with 50% (*R*)-3HB (ata-P[50%(*R*)-3HB]), and investigate the stereochemical and morphological effects of enzymatic degradation of binary blends of bacterial P[(*R*)-3HB] with three chemosynthetic P[(*R*,*S*)-3HB] samples. The physical properties of the polymer blends are studied by means of differential scanning calorimetry, X-ray diffraction, and optical microscopy. The enzymatic degradabilities are examined with PHB depolymerase from *P. pickettii*,[13] and the water-soluble products during the enzymatic degradation of blend films are characterized by HPLC analysis. The mechanism of enzymatic degradation of P(3HB) films is discussed.

Experimental Section

Materials. 1-Ethoxy-3-chlorotetrabutyldistannoxane catalyst was prepared along the literature method,[43] and the procedures of synthesis were reported in a previous paper.[40] A $Zn(C_2H_5)_2/H_2O$ (1/0.6) catalyst was prepared by a reported method.[21] (*R*)-β-Butyrolactone[36] (e.e. 92%) ((*R*)-β-BL) and racemic (*R*,*S*)-β-butyrolactone ((*R*,*S*)-β-BL) were dried by CaH_2 and distilled under reduced pressure. The enantiomeric excess of (*R*)-β-BL was determined to be 92% by HPLC analysis.[40] Racemic β-BL was purchased from Aldrich Chemical Co.

Synthesis of P(3HB) Samples. Bacterial poly[(*R*)-3-hydroxybutyrate] (P[(*R*)-3HB]) was produced from butyric acid by *Alcaligenes eutrophus*.[44] Poly[(*R*,*S*)-3-hydroxybutyrate] (P[(*R*,*S*)-3HB]) stereoisomer samples with different stereoregularities were synthesized by the ring-opening polymerization of (*R*)-β-BL with (*R*,*S*)-β-BL in the presence of 1-ethoxy-3-chlorotetrabutyldistannoxane[36] or $ZnEt_2/H_2O$[21] as a catalyst. The polymerization of β-butyrolactone with 1-ethoxy-3-chlorotetrabutyldistannoxane was carried out without solvent at 100 °C for 4 h under argon atmosphere.[40] The polymerization of β-butyrolactone with $ZnEt_2/H_2O$ was carried out in 1,2-dichloroethane at 60 °C for 5 days under nitrogen atmosphere.[33] The produced P[(*R*,*S*)-3HB] was dissolved in chloroform and precipitated in a mixture of diethyl ether and hexane (1/3). The precipitate was dried in vacuo at room temperature.

Preparation of Blend Films. Blend films (0.1 mm thickness) of bacterial P[(*R*)-3HB] with chemosynthetic P[(*R*,*S*)-3HB] were prepared by solvent-casting techniques from chloroform solutions of P(3HB) using glass Petri dishes as casting surfaces. The blend films were then aged at least 3 weeks at room temperature to reach equilibrium crystallinity prior to analysis. The amorphous P[(*R*,*S*)-3HB] polymer was solution cast onto a Teflon sheet producing films of 0.1 mm thickness, and used for analysis.

Enzymatic Degradation. The extracellular PHB depolymerase from *P. pickettii* was purified to electrophoretic homogeneity by the methods of Yamada *et al.*[13] The enzymatic degradation of blend films by the purified PHB depolymerase was carried out at 37 °C in 0.1 M potassium phosphate buffer (pH 7.4). The blend films (initial weights, 14 mg; initial film dimensions, 10 × 10 × 0.1 mm) were placed in small bottles containing 1.0 mL of the buffer. The reaction was started by the addition of 10 μL of an aqueous solution of PHB depolymerase (2 μg). For the weight loss measurement of films, the reaction solution was incubated for 3 h at 37 ± 0.1 °C with shaking, and the sample films were removed after the reaction, washed with distilled water, and dried to constant weight in vacuo before analysis. The values of weight loss of the blend films for 3 h were in the range of 0−3 mg, depending on the fraction of P[(*R*,*S*)-3HB] components in blend. The weight loss data were averaged on three film samples. The water-soluble products after enzymatic degradation of P(3HB) films were examined by HPLC analysis of the reaction solution.

The rate of 3-hydroxybutyrate (3HB) units liberation from a blend film during the enzymatic degradation was determined by a UV method of absorbance measurement at 210 nm of phosphate buffer containing water-soluble products as described in a previous paper.[45] In this method, the amounts of monomer and oligomers of 3-hydroxybutyric acid generated as water-soluble products during the course of enzymatic degradation of blend film were measured by monitoring the increase in absorbance at 210 nm on a spectrophotometer. In this experiment, the enzyme solution (10 μL) of PHB depolymerase (2.0 μg) was added to the reaction cuvette containing 1.0 mL of 0.1 M potassium phosphate buffer (pH 7.4). The cuvette was maintained at 37 °C. The enzymatic degradation was started by the addition of blend film (initial film dimension, 10 × 10 × 0.1 mm), and the absorbance at 210 nm *vs*

time was monitored continuously on a Hitachi U-2000 spectrophotometer. The amount of 3HB units in the water-soluble products liberated from blend film by the enzymatic reaction was calculated using the absorption coefficient of 95 M^{-1} cm^{-1} at 210 nm for 3-hydroxybutyric acid at 37 °C. The absorption coefficients at 210 nm of monomer and dimer of 3-hydroxybutyric acid were found to be 95 and 190 M^{-1} cm^{-1} at 37 °C, respectively. The absorption coefficient (95 M^{-1} cm^{-1}) of (*R*)-3-hydroxybutyric acid (Takasago International Co.) was determined at 37 °C in 0.1 M potassium phosphate buffer (pH 7.4), and the absorbance at 210 nm was verified to be proportional to the concentration of (*R*)-3-hydroxybutyric acid in the range of 0−10 mM. As will be shown in Figure 6, the enzymatic degradation of bacterial P[(*R*)-3HB] produced a mixture of monomer and dimer of (*R*)-3-hydroxybutyric acid. The degradation product was fractionated into the monomer and dimer by HPLC (column, LiChrospher RP-8). The dimer of (*R*)-3-hydroxybutyric acid (^{1}H NMR (at 400 MHz in D_2O) δ 1.21 (d, 3H), 1.30 (d, 3H), 2.45−2.66 (m, 4H), 4.22 (m, 1H), 5.26 (m, 1H)) was collected and used for the determination of the absorption coefficient (190 M^{-1} cm^{-1}) at 37 °C in 0.1 M potassium phosphate buffer. The absorption coefficients of trimer and tetramer were not determined. In this study, the absorption coefficient (95 M^{-1} cm^{-1} at 37 °C) of (*R*)-3-hydroxybutyric acid at 210 nm was used to calculate the amounts of 3-hydroxybutyrate units produced as water-soluble products, on the assumption that the absorption coefficient of 3-hydroxybutyrate units is independent of the chain length.

Analytical Procedures. All molecular weight data were obtained by gel-permeation chromatography at 40 °C, using a Shimadzu 6A GPC system and a 6A refractive index detector with Shodex K-80M and K-802 columns. Chloroform was used as eluent at a flow rate of 0.8 mL/min, and sample concentrations of 1.0 mg/mL were applied. The number-average and weight-average molecular weights (M_n and M_w) were calculated by using a Shimadzu Chromatopac C-R4A equipped with a GPC program. A molecular weight calibration curve of P(3HB) was obtained on the basis of the universal calibration method[46] with polystyrene standards of low polydispersities.

The ^{13}C NMR spectra at 100 MHz of P(3HB) polymers were recorded on a JEOL Alpha-400 spectrometer at 27 °C in a $CDCl_3$ solution of polymer (20 mg/mL) with a 5.5 ms pulse width (45° pulse angle), 5 s pulse repetition, 25000 Hz spectral width, 64K data points, and 13000 accumulations.

Differential scanning calorimetry (DSC) data of blends were recorded in the temperature range −150 to 200 °C on a Shimadzu DSC-50 equipped with a cooling accessory under a nitrogen flow of 30 mL/min. Samples of 10 mg were encapsulated in aluminum pans and heated from 0 to 200 °C at a rate of 10 °C/min. The peak melting temperature (T_m) and enthalpy of fusion (ΔH_m) were determined from the DSC endotherms. For measurement of the glass-transition temperature (T_g), the samples were maintained at 200 °C for 1 min and then rapidly quenched at −150 °C. They were heated from −150 to 200 °C at a heating rate of 20 °C/min. The T_g was taken as the midpoint of the heating capacity change. For the DSC measurement of the equilibrium melting temperatures (T_m^0), the melt films of blends were isothermally crystallized at different crystallization temperature (T_c) for 12 h after melting at 200 °C for 30 s.

The morphologies of P[(*R*)-3HB] spherulites of P[(*R*)-3HB]/P[(*R*,*S*)-3HB] blends were observed with a Nikon optical microscope equipped with crossed polarizers and a Linkham hot stage. The films (2 mg) of P[(*R*)-3HB]/P[(*R*,*S*)-3HB] blends, as obtained by solvent casting, were first heated on a hot stage from room temperature to 200 °C at a rate of 30 °C/min. Samples were maintained at 200 °C for 30 s and then the temperature was rapidly lowered to a given crystallization temperature (T_c) of 60−120 °C. The samples were crystallized isothermally at a given T_c to monitor the growth of the spherulites as function of time. The radial growth rate of P[(*R*)-3HB] spherulites was calculated as the slope of the line obtained by plotting the spherulite radius against time with more than 10 data points. For each crystallization measurement, the radial growth rate of the different three spherulites were recorded under the same conditions, and the spherulitic growth rates were averaged. During the thermal treatment, the P[(*R*)-3HB]/P[(*R*,*S*)-3HB] blend films were kept under nitrogen flow in order to limit the degradation of the polymer. In order to minimize the risk of thermal degradation of P[(*R*)-3HB]/P[(*R*,*S*)-3HB] blends, a new sample was used for each crystallization measurement.

The stress−strain curves of solution-cast films of P[(*R*)-3HB]/P[(*R*,*S*)-3HB] blends were obtained at 23 °C at a strain rate of 20 mm/min on an Imada tensile machine (model SV-50). The specimens were dogbone-shaped according to JIS K 7127, their prismatic part measuring 25 × 5 × 0.1 mm. At least five samples were measured and the mechanical tensile data were determined from such curves on average of three specimens using an extensometer.

The X-ray diffraction patterns of films were recorded at 27 °C on a Rigaku RAD-IIIB system using nickel-filtered Cu Kα radiation (λ = 0.154 nm; 40 kV; 30 mA) in the 2θ range 6−40° at a scan speed of 2.0 deg/min. Degrees of crystallinity (X_c) of P[(*R*)-3HB]/P[(*R*,*S*)-3HB] blends were calculated from diffracted intensity data according to Vonk's method.[47]

The surfaces of blend films were observed with a scanning electron microscope (JEOL JSM-5300) after gold coating of the films using an ion coater.

The water-soluble products after enzymatic degradation of blend films were analyzed by using a Shimadzu LC-9A HPLC system with a gradient controller and a SPD-10A UV spectrophotometric detector. The stainless steel column (250 × 4 mm) containing LiChrospher RP-8 (5 μm) was used at 40 °C. Sample solutions after the enzymatic degradation were acidified to pH 2.5 with HCl solution, and 50 μL solutions were injected. The gradient of distilled water (pH 2.5, adjusted by the addition of HCl solution) to acetonitrile for 40 min was carried out with pump speed of 1.0 mL/min. The monomer and oligomers of 3-hydroxybutyric acid were detected at 210 nm. The amounts of monomer and oligomers of 3HB units in the water-soluble products were calculated from the peak areas of HPLC patterns, on the assumption that the absorption coefficients at 210 nm of oligomers were proportional to the number of 3HB units in oligomers. The monomer, dimer, and trimer in degradation product of P[(*R*)-3HB]/ata-P[50%(*R*)-3HB] = 25/75 (w/w) blend film were fractionated by HPLC for ^{1}H NMR analysis. Each product was collected from HPLC eluate, and the solvent was evaporated. The 400 MHz ^{1}H NMR spectra were recorded in D_2O: (dimer) δ 1.21 (d, 3H), δ 1.30 (d, 3H), δ 2.45−2.66 (m, 4H), 4.22 (m, 1H), 5.26 (m, 1H); (trimer) δ 1.21−1.32 (m, 9H), δ 2.38−2.69 (m, 6H), 4.21 (m, 1H), 5.19 (m, 1H), 5.28 (m, 1H). Tetramer of 3-hydroxybutyric acid in the water-soluble product could not be fractionated due to a low concentration.

Results and Discussion

Preparation of Polymers. Bacterial P[(*R*)-3HB] was produced from butyric acid by *A. eutrophus*. P[(*R*,*S*)-3HB] stereoisomers were synthesized by the stereocopolymerization of (*R*,*S*)-β-BL with (*R*)-β-BL in the presence of 1-ethoxy-3-chlorotetrabutyldistannoxane or $ZnEt_2/H_2O$ as a catalyst. Table 1 shows the mole ratios of (*R*)- and (*S*)-β-BL monomers used for stereocopolymerization, the number-average molecular weights (M_n), the polydispersities (M_w/M_n), and the isotactic diad fractions ([*i*]) of produced polymers. The [*i*] values were determined from the relative peak areas of carbonyl carbon resonances in ^{13}C NMR spectra of polymers.[35] The [*i*] values were 0.46 and 0.30 for the P[(*R*,*S*)-3HB] samples produced at monomer feed ratio of (*R*)-/(*S*)-β-BL = 70/30 and 50/50 with a distannoxane catalyst, respectively. The P[(*R*,*S*)-3HB] sample produced at monomer feed ratio of (*R*)-/(*S*)-β-BL = 50/50 with $Zn(C_2H_5)_2/H_2O$ catalyst has the [*i*] value of 0.51. It was reported that both the distannoxane[36] and $Zn(C_2H_5)_2/H_2O$[33] catalysts proceeded the ring-opening polymerization of β-BL by breaking the bond between carbonyl

Table 1. Molecular Weights and Isotactic Fractions of P(3HB) Samples

sample	monomer feed ratio, *R*/*S*	polymer yield, %	molecular weight $M_n \times 10^{-3}$	molecular weight M_w/M_n	isotactic diad fraction,[e] [*i*]
P[100%(*R*)-3HB][a]	–	–	281	2.3	1.00
ata-P[70%(*R*)-3HB][b]	70/30	90	105	1.8	0.46
syn-P[50%(*R*)-3HB][c]	50/50	99	145	1.8	0.30
ata-P[50%(*R*)-3HB][d]	50/50	97	20	1.2	0.51

[a] Bacterial P[(*R*)-3HB]. [b] Atactic P[(*R*,*S*)-3HB] with 70% (*R*)-3HB was synthesized by polymerization of (*R*)- and (*S*)-β-BL (*R*/*S* = 70/30) with 1-ethoxy-3-chlorotetrabutyldistannoxane as a catalyst. Polymerization conditions: mole ratio of catalyst/monomer =1/4000, reaction temperature = 100 °C, reaction time = 4 h, without solvent. [c] Syndiotactic P[(*R*,*S*)-3HB] with 50% (*R*)-3HB was synthesized by polymerization of racemic β-BL with 1-ethoxy-3-chlorotetrabutyldistannoxane as a catalyst. Polymerization conditions: mole ratio of catalyst/monomer = 1/4000, reaction temperature = 100 °C, reaction time = 4 h, without solvent. [d] Atactic P[(*R*,*S*)-3HB] with 50% (*R*)-3HB was synthesized by polymerization of racemic β-BL with $Zn(C_2H_5)_2/H_2O$ as a catalyst. Polymerization conditions: mole ratio of catalyst/monomer = 1/25, reaction tempeorature = 60 °C, reaction time = 5 days, in CH_2Cl_2. [e] Determined from carbonyl carbon resonance in ^{13}C NMR spectra.

Table 2. Thermal Properties and X-ray Crystallinities of Solution-Cast P[(*R*)-3HB]/P[(*R*,*S*)-3HB] Blend Films

sample	blend composition, wt ratio	T_g,[a] °C	T_m,[b] °C	ΔH_m,[c] J/g	T_m^0,[d] °C	X_c,[e] %
P[(*R*)-3HB]		5	177	90	191	62 ± 5
P[(*R*)-3HB/ata-P[70%(*R*)-3HB]	75/25	5	176	44	186	45 ± 5
			160	8		
	50/50	5	174	37	182	25 ± 5
			158	8		
	25/75	6	172	27	174	14 ± 5
			154	5		
	0/100	6		0		0
P[(*R*)-3HB]/syn-P[50%(*R*)-3HB]	75/25	5	176	75	187	48 ± 5
			161	7		
	50/50	5	175	32	183	35 ± 5
			159	9		
	25/75	5	173	22	180	22 ± 5
			157	6		
			50	3		
	0/100	6	52	26		26 ± 5
			62			
P[(*R*)-3HB/ata-P[50%(*R*)-3HB]	75/25	4	174	50		49 ± 5
			160	6		
	50/50	4	173	44		30 ± 5
			157	7		
	25/75	4	173	22		13 ± 5
			157	3		
	0/100	7	–	0		0

[a] Glass-transition temperature; measured by DSC (second scan) from −150 to 200 °C at a rate of 20 °C/min. [b] Melting temperature; measured by DSC (first scan) from 0 to 200 °C at a rate of 10 °C/min. [c] Enthalpy of fusion; measured by DSC (first scan). [d] Equilibrium melting temperature; determined from Hoffman−Weeks plots. [e] Degree of crystallinity; determined from X-ray diffraction patterns.

carbon and oxygen atoms of β-BL ring (acyl cleavage) with retention of the configuration. Therefore, the three types of P[(*R*,*S*)-3HB] samples with [*i*] = 0.46, 0.30, and 0.51 are termed as atactic P[(*R*,*S*)-3HB] with 70% (*R*)-3HB (ata-P[70%(*R*)-3HB]), syndiotactic P[(*R*,*S*)-3HB] with 50% (*R*)-3HB (syn-P[50%(*R*)-3HB]), and atactic P[(*R*,*S*)-3HB] with 50% (*R*)-3HB (ata-P[50%(*R*)-3HB]), respectively.

Physical Properties of Blends. The glass-transition temperature (T_g), peak melting temperature (T_m), and enthalpy of fusion (ΔH_m) of solvent-cast blend films were determined from DSC thermograms. The results are given in Table 2. The T_g values of all blends were observed at 5 ± 2 °C, independent of the blend compositions. Two atactic samples of ata-P[70%(*R*)-3HB] and ata-P[50%(*R*)-3HB] were completely amorphous and showed no fusion. The predominantly syndiotactic sample of syn-P[50%(*R*)-3HB] had two endothermic peaks at around 52 and 62 °C, and the degree of crystallinity was 26 ± 5%. All of P[(*R*)-3HB]/P[(*R*,*S*)-3HB] blends studied in this work had two endothermic peaks at temperatures of 150−180 °C. Both T_m values slightly decreased as the fraction of chemosynthetic P[(*R*,*S*)-3HB] component was increased. In order to see whether the two peaks arise from a recrystallization process, the DSC curves of polymer blends were recorded at different heating rates of 5 to 40 °C/min. As the heating rate is increased, the higher temperature peak became smaller while the lower temperature peak remained almost unaltered. The result suggests that higher melting endothermic peak is caused by the rearrangement of the initial crystal morphology of P[(*R*)-3HB]. For the P[(*R*)-3HB]/syn-P[50%(*R*)-3HB] blends of 75/25 and 50/50 weight ratios, no endothermic peak of syndiotactic component was detected at temperatures below 100 °C. This indicates that syn-P[50%(*R*)-3HB] component was not crystallized in the presence of P[(*R*)-3HB] component. However, a broad endothermic peak was observed at around 50 °C for the P[(*R*)-3HB]/syn-P[50%(*R*)-3HB] blend of 25/75 weight ratio, and the ΔH_m value was less than 3 J/g. The ΔH_m values of binary blends decreased from 90 to 30 ± 5 J/g with increasing the P[(*R*,*S*)-3HB] content in the blend films.

The T_m values of binary blends crystallized isothermally at different temperatures from melt were measured by DSC. The plots of T_m against crystallization temperature (T_c) show almost linear trend for all blend compositions. The Hoffman−Weeks equation fits the experimental data quite well. The equilibrium melting temperature (T_m^0) was determined by the extrapolation of T_m values to the line of $T_m = T_c$.[48] The values of T_m^0 are listed in Table 2. The T_m^0 value of binary blends

Table 3. Mechanical Properties at 23 °C for Solution-Cast Films of P[(*R*)-3HB/P[(*R*,*S*)-3HB] Blends

sample	blend composition, wt ratio	Young's modulus, MPa	tensile strength, MPa	elongation to break, %
P[(*R*)-3HB]		1560 ± 100	38 ± 3	5 ± 1
P[(*R*)-3HB]/ata-P[70%(*R*)-3HB]	75/25	350 ± 20	26 ± 3	150 ± 10
	50/50	210 ± 10	14 ± 1	320 ± 30
	25/75	32 ± 5	6 ± 1	580 ± 50
P[(*R*)-3HB]/syn-P[50%(*R*)-3HB]	75/25	540 ± 30	30 ± 3	30 ± 5
	50/50	340 ± 20	8 ± 1	67 ± 10
	25/75	25 ± 5	15 ± 1	680 ± 50
	0/100	20 ± 5	13 ± 1	1020 ± 70
P[(*R*)-3HB]/ata-P[50%(*R*)-3HB]	75/25	260 ± 15	20 ± 2	210 ± 20
	50/50	180 ± 10	10 ● 1	380 ± 30
	25/75	25 ± 5	3 ± 1	620 ± 60

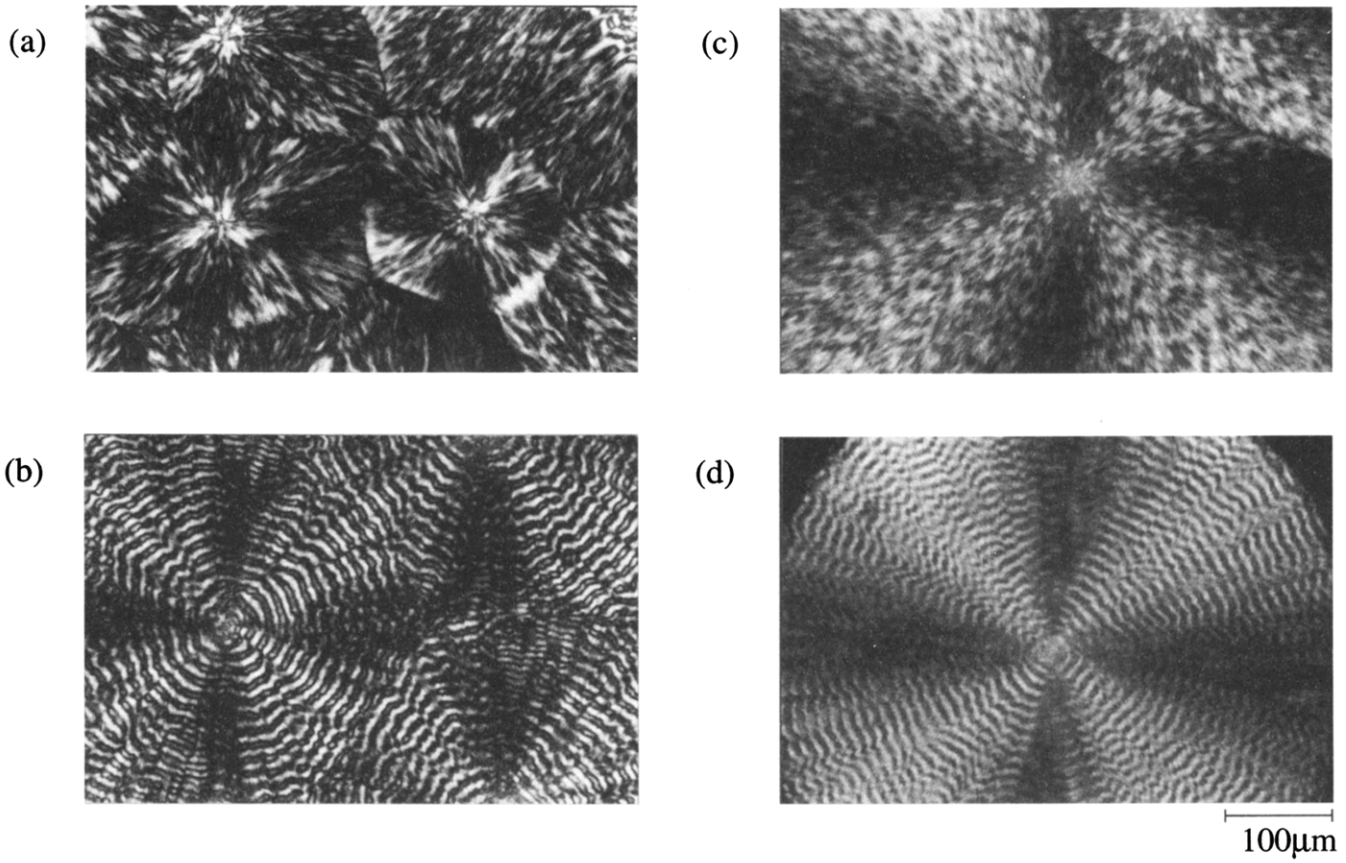

Figure 1. Optical micrographs of P[(*R*)-3HB] spherulites for P[(*R*)-3HB]/ata-P[70%(*R*)-3HB] = 50/50 (w/w) blend film grown isothermally at (a) T_c = 70 °C and (b) T_c = 110 °C, and for P[(*R*)-3HB]/syn-P[50%(*R*)-3HB] = 50/50 (w/w) blend film grown isothermally at (c) T_c = 70 °C and (d) T_c = 110 °C.

decreased from 191 to 174 °C as the P[(*R*,*S*)-3HB] content was increased from 0 to 75 wt %. The melting temperature depression of the P[(*R*)-3HB] polymer by blending with the chemosynthetic P[(*R*,*S*)-3HB] polymer suggests that the P[(*R*)-3HB] and P[(*R*,*S*)-3HB] polymers are miscible in the melt, as reported in a previous paper[41] for the binary blends of P[(*R*)-3HB]/ata-P[50%-(*R*)-3HB].

The degrees of X-ray crystallinity (X_c) of blend films are listed in Table 2. The X_c values of P[(*R*)-3HB]/ata-P[70%(*R*)-3HB] and P[(*R*)-3HB]/ata-P[50%(*R*)-3HB] blend films decreased from 62 to 14% as the content of atactic P[(*R*,*S*)-3HB] components was increased from 0 to 75 wt %. For the P[(*R*)-3HB]/syn-P[50%(*R*)-3HB] blend films, the X_c values also decreased with an increase in the content of syn-P[50%(*R*)-3HB] component.

Table 3 lists the mechanical properties of solution-cast films of P[(*R*)-3HB]/P[(*R*,*S*)-3HB] blends. The Young's modulus and tensile strength at 23 °C of blend films were reduced with increasing the fraction of P[(*R*,*S*)-3HB] components. In contrast, the elongation to break of films were increased from 5 to over 500% as the fraction of chemosynthetic P[(*R*,*S*)-3HB] components was increased from 0 to 75 wt %. The result indicates that the P[(*R*)-3HB]/P[(*R*,*S*)-3HB] blend films become soft and flexible as the fraction of P[(*R*,*S*)-3HB] components are increased.

The growth of P[(*R*)-3HB] spherulites in P[(*R*)-3HB]/P[(*R*,*S*)-3HB] blends was observed with a polarized optical microscope. Blend samples were isothermally crystallized at a given temperature after melting at 200 °C for 30 s. Figure 1 shows typical optical micrographs of P[(*R*)-3HB] spherulites for P[(*R*)-3HB]/ata-P[70%(*R*)-3HB] [50/50 (w/w)] crystallized at 70 and 110 °C and for P[(*R*)-3HB]/syn-P[50%(*R*)-3HB] [50/50 (w/w)] crystallized at 70 and 110 °C. There was no evident slowing of the growth fronts as the spherulites impinge. The spherulite radius increased linearly with time. The radial growth rate depended on both the crystallization temperature and the blend composition. After crystal-

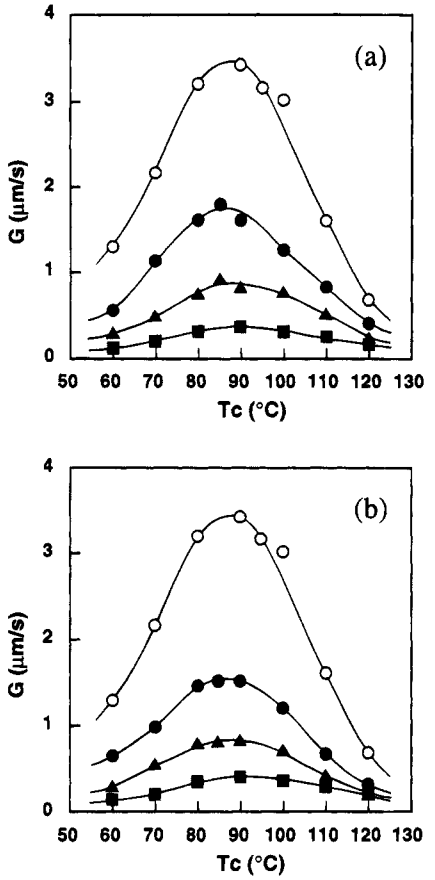

Figure 2. The radial growth rate (G) of P[(R)-3HB] spherulite at various crystallization temperatures (T_c) for (a) P[(R)-3HB]/ata-P[70%(R)-3HB] blend and (b) P[(R)-3HB]/syn-P[50%(R)-3HB] blend: (○) P[(R)-3HB]/P[(R,S)-3HB] = 100/0; (●) 75/25; (▲) 50/50; (■) 25/75 (w/w).

lization, uniform spherulites were well-developed throughout the blend film, and no apparent evidence of phase separation of P[(R,S)-3HB] components was detected, even at the highest concentration of P[(R,S)-3HB] (75 wt %). These results indicate that P[(R,S)-3HB] components exist within the spherulites of P[(R)-3HB].

Figure 2, parts a and b, show the radial growth rate (G) of P[(R)-3HB] spherulites at different crystallization temperatures for blends with ata-P[70%(R)-3HB] and with syn-P[50%(R)-3HB], respectively. The radial growth rate (G) was calculated as the slope of the line obtained by plotting the spherulite radius against time. A maximum value (3.4 μm/s) of G was observed near 90 °C for bacterial P[(R)-3HB] homopolymer. The G values decreased with an increase in the content of P[(R,S)-3HB] component for both blends of P[(R)-3HB]/ata-P[70%(R)-3HB] and P[(R)-3HB]/syn-P[50%(R)-3HB]. The temperature of peak growth rate was largely unaffected since addition of P[(R,S)-3HB] did not decrease the glass-transition temperature of the blend. The results suggest that the P[(R,S)-3HB] components are able to act as a diluent for crystallizable P[(R)-3HB]. The same result was obtained for the blends of P[(R)-3HB]/ata-P[50%(R)-3HB].[41]

Enzymatic Degradation of Blend Films. Enzymatic degradation of blend films were carried out at 37 °C in 0.1 M potassium phosphate buffer (pH 7.4) containing 2 μg of purified PHB depolymerase from *P. pickettii*. Sample films were prepared by solution-casting techniques from chloroform solutions of binary blends. The water-soluble products were quantitatively

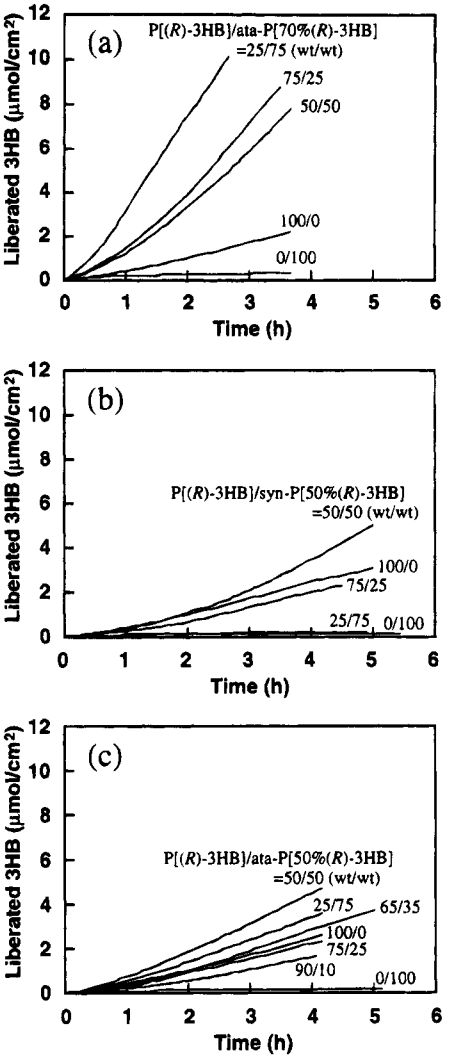

Figure 3. The amounts of 3HB units liberated as water-soluble products during the enzymatic degradation of P[(R)-3HB]/P[(R,S)-3HB] blend films in 0.1 M potassium phosphate solution (pH 7.4) containing PHB depolymerase (2.0 μg/mL) from *P. pickettii* at 37 °C: (a) P[(R)-3HB]/ata-P[70%(R)-3HB] blend, (b) P[(R)-3HB]/syn-P[50%(R)-3HB] blend, and (c) P[(R)-3HB]/ata-P[50%(R)-3HB] blend.

detected by monitoring the absorption at 210 nm due to the carbonyl groups of 3HB units in products on a spectrophotometer.[45] Figure 3 shows the time-dependent changes in the absorbance of reaction solution at 210 nm, caused by the liberation of 3HB units during the enzymatic degradation of blend films. The amount of 3HB units liberated as water-soluble products was calculated using the absorption coefficient of 95 M^{-1} cm^{-1} at 210 nm of 3-hydroxybutyric acid, on the assumption that the absorption coefficients at 210 nm of oligomers are proportional to the number of 3HB units in oligomers. The rates of 3HB generation were slow for 30 min at the initial stage of enzymatic degradation, but the amounts of 3HB units liberated from blend films increased proportionally with time after 30 min. The rate of enzymatic degradation was then determined from the linear dependence of the amount of liberated 3HB units against time.

Figure 4 shows the production rate of 3HB units liberated as water-soluble products from blend films as a function of the weight content of chemosynthetic P[(R,S)-3HB] components in the blends, together with the weight loss rate of blend films by PHB depolymerase. Both the kinetic data of UV and weight loss

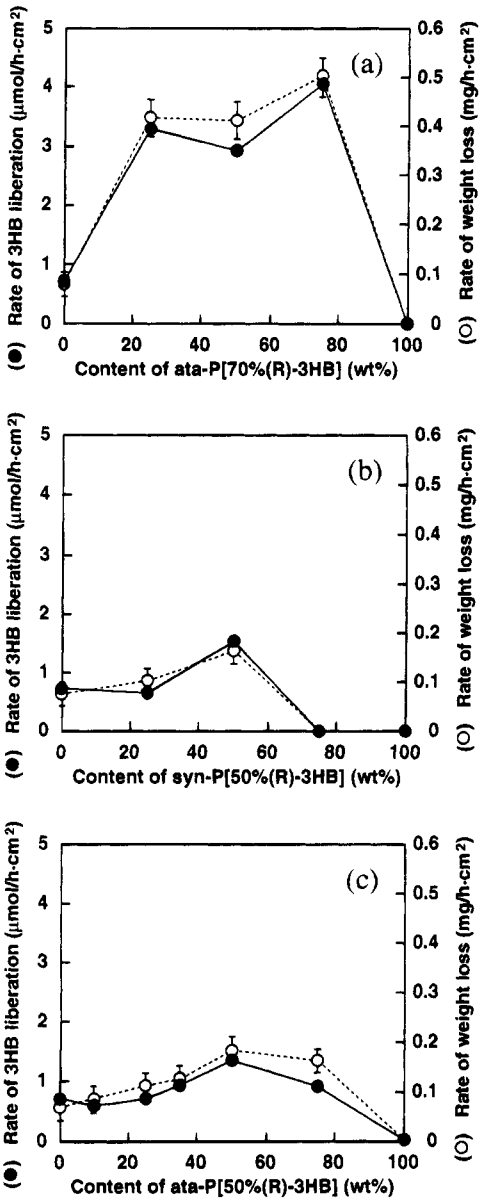

Figure 4. The rates of 3HB liberation as water-soluble products (●) and of weight loss (○) of P[(*R*)-3HB]/P[(*R*,*S*)-3HB] blend films during the enzymatic degradation in 0.1 M potassium phosphate solution (pH 7.4) containing PHB depolymerase (2.0 μg/mL) from *P. pickettii* at 37 °C: (a) P[(*R*)-3HB]/ata-P[70%(*R*)-3HB] blend, (b) P[(*R*)-3HB]/syn-P[50%(*R*)-3HB] blend, and (c) P[(*R*)-3HB]/ata-P[50%(*R*)-3HB] blend. The weight loss data were averaged on three film samples.

measurements show almost the same dependence of P[(*R*,*S*)-3HB] contents on the rate of enzymatic degradation. The rates of enzymatic degradation of P[(*R*)-3HB]/ata-P[70%(*R*)-3HB] blend films were higher than that of bacterial P[(*R*)-3HB] homopolymer. The highest rate of enzymatic degradation was observed at 75 wt % of ata-P[70%(*R*)-3HB], and the rate was about 5 times faster than that of P[(*R*)-3HB] homopolymer film. A very slow rate of enzymatic degradation was observed on the film of ata-P[70%(*R*)-3HB] homopolymer.[40] For the P[(*R*)-3HB]/syn-P[50%(*R*)-3HB] blend films, the rate of enzymatic degradation also increased as the content of syn-P[50%(*R*)-3HB] was increased 0 to 50 wt %. However, little enzymatic degradation took place on the surface of the blend films of P[(*R*)-3HB/syn-P[50%(*R*)-3HB] = 25/75 (w/w). The rates of enzymatic degradation for P[(*R*)-3HB]/ata-P[50%(*R*)-3HB] blend films were also higher than those of P[(*R*)-3HB] and ata-P[50%-(*R*)-3HB] homopolymers. The highest rate was observed at 50 wt % of ata-P[50%(*R*)-3HB], and the rate was about twice faster than that of P[(*R*)-3HB] film.

Figure 5 shows the scanning electron micrographs (SEMs) of the surface of and a cross section of P[(*R*)-3HB]/P[(*R*,*S*)-3HB] blend films after enzymatic degradation. The surfaces of blend films after enzymatic degradation were apparently blemished by the function of depolymerase, while no change took place inside the films, indicating that the enzymatic degradation occurred on the surface of films. No phase-separated morphologies were detected in SEMs of the cross section of blend films.

In previous papers,[18,27] we reported that the rate of enzymatic degradation of bacterial P[(*R*)-3HB] film increased with a decrease in the crystallinity and that a PHB depolymerase first hydrolyzed the P[(*R*)-3HB] chains in an amorphous state on the surface of film. In addition, we suggested that the rate of enzymatic degradation for P[(*R*)-3HB] chains in an amorphous state was about 20 times higher than the rate for P[(*R*)-3HB] chains in a crystalline state. The acceleration of enzymatic degradation for P[(*R*)-3HB]/P[(*R*,*S*)-3HB] blend films may be caused by the decrease in crystallinity.

HPLC Analysis of Water-Soluble Products. In a previous paper,[40] we demonstrated that the enzymatic hydrolysis of bacterial P[(*R*)-3HB] film by PHB depolymerases produced a mixture of monomer and dimer of 3-hydroxybutyric acid as water-soluble products, while that of the enzymatic hydrolysis of chemosynthetic P[(*R*,*S*)-3HB] films produced trimer and tetramer in addition to monomer and dimer. In this study, we measured the composition of water-soluble products after the enzymatic degradation of P[(*R*)-3HB]/P[(*R*,*S*)-3HB] blend films by HPLC analysis. The enzymatic degradations of blend films were carried out at 37 °C in 0.1 M potassium phosphate buffer (pH 7.4) of 1 mL containing a PHB depolymerase (2 μg) from *P. pickettii*. The reaction solutions were collected after enzymatic degradation and analyzed by a high-performance liquid chromatography (HPLC). The relative amounts of 3HB unit in water-soluble products were determined from peak areas in HPLC curves.

Figure 6 shows the weight distribution of water-soluble products after enzymatic degradation of P[(*R*)-3HB]/P[(*R*,*S*)-3HB] blend films for 3 h. The HPLC curve of products from bacterial P[(*R*)-3HB] showed only two peaks, arising from monomer and dimer of (*R*)-3-hydroxybutyric acid. In contrast, the binary blend films containing P[(*R*,*S*)-3HB] components gave trimer and tetramer of 3-hydroxybutyric acid as products in addition to monomer and dimer, and the fractions of trimer and tetramer increased with an increase in the composition of chemosynthetic P[(*R*,*S*)-3HB].

In a previous paper,[40] we reported that the rates of enzymatic degradation of the films of chemosynthetic P[(*R*,*S*)-3HB] stereoisomers ranging in the [*i*] value from 0.68 to 0.92 were higher than that of bacterial P[(*R*)-3HB], and that the stereoirregular P(3HB) samples produced a mixture of monomer, dimer, trimer, and tetramer of 3HB unit as water-soluble products. As shown in Figures 3 and 4, atactic and syndiotactic P[(*R*,*S*)-3HB] samples were hardly hydrolyzed by PHB depolymerase from *P. pickettii*. However, when bacterial P[(*R*)-3HB] was blended with atactic and syndiotactic P[(*R*,*S*)-3HB], the enzymatic erosion of films was accelerated (Figures 3 and 4), and the trimer and

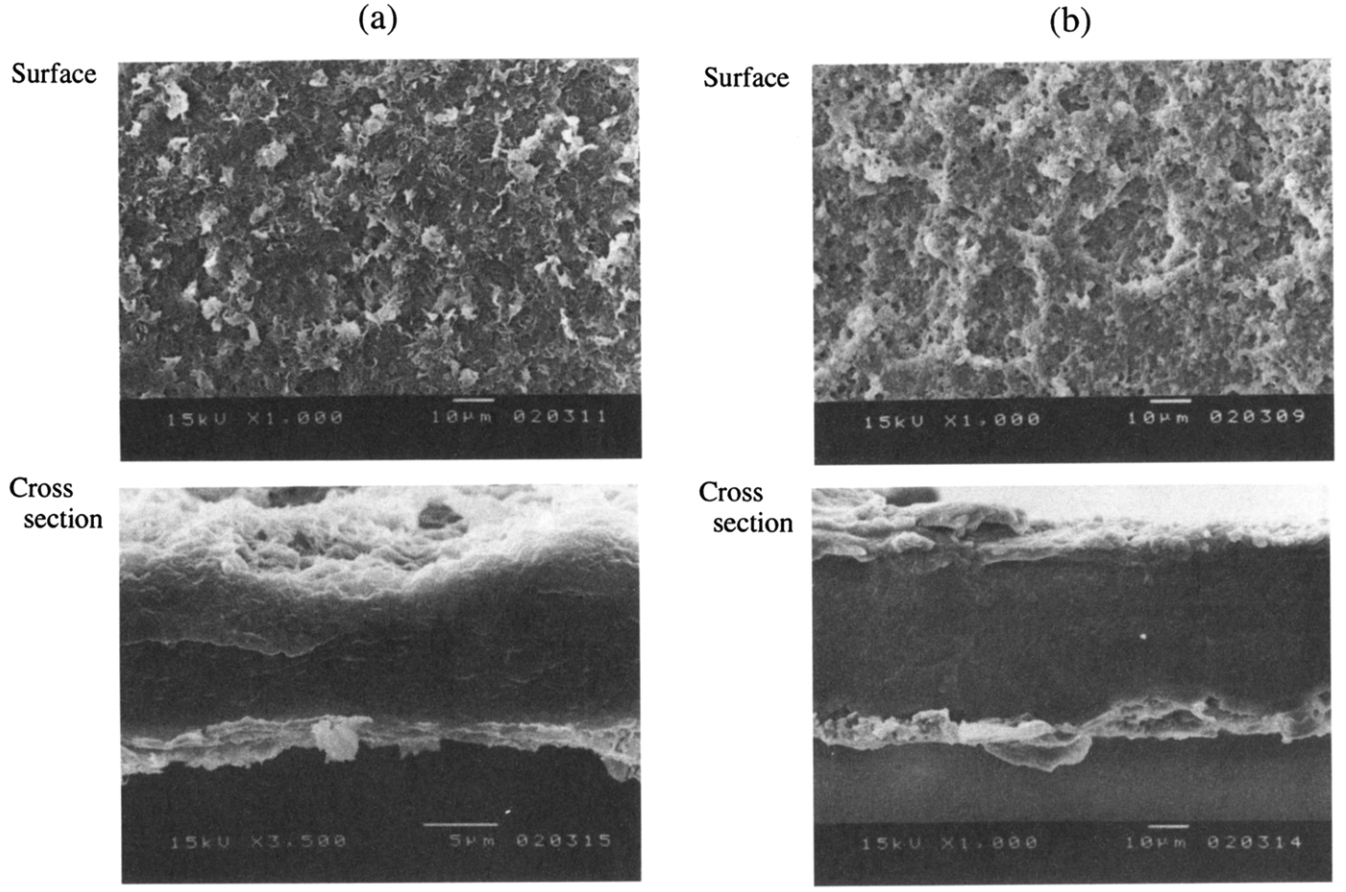

Figure 5. The scanning electron micrographs (SEMs) of the surfaces and cross sections of P[(*R*)-3HB]/P[(*R*,*S*)-3HB] blend films after enzymatic degradation with PHB depolymerase (2.0 μg/mL) from *P. pickettii* at 37 °C: (a) surface and cross section of P[(*R*)-3HB]/ata-P[70%(*R*)-3HB] = 50/50 (w/w) blend film (weight loss 30%) degraded for 5 h, and (b) surface and cross section of P[(*R*)-3HB]/syn-P[50%(*R*)-3HB] = 75/25 (w/w) blend film (weight loss 18%) degraded for 12 h.

tetramer of 3HB unit were produced in addition to monomer and dimer as water-soluble products (Figure 6). The data of thermal properties (Table 2) and crystallization (Figures 1 and 2) of polymer blends of P[(*R*)-3HB] with atactic and syndiotactic P[(*R*,*S*)-3HB] indicate that atactic and syndiotactic P[(*R*,*S*)-3HB] are miscible with P[(*R*)-3HB] in the melt and in the amorphous regions. These results suggest that atactic and syndiotactic P[(*R*,*S*)-3HB] components are hydrolyzed by PHB depolymerase in the presence of P[(*R*)-3HB] component, and that the trimer and tetramer are produced by the enzymatic hydrolysis of P[(*R*,*S*)-3HB] components.

Modeling of Enzymatic Degradation of P(3HB) Film. Saito *et al.*[49-51] have demonstrated that the PHB depolymerase (MW 47 kDa) of *A. faecalis* has a hydrophobic domain (5 kDa) as a binding site to adhere to the hydrophobic surface of P[(*R*)-3HB] film, in addition to a catalytic domain as an active site. Such binding domains adsorbing on the surface of polymeric materials have been found in other enzymes capable of depolymerizing water-insoluble substrates such as cellulase,[52] chitinase,[53,54] and xylanase.[52,55] Jendrossek *et al.*[56] have reported that several PHB depolymerases contain a terminal sequence homologous to that of *A. faecalis*. The presence of binding and catalytic domains in depolymerizing enzymes suggests that the enzymatic degradation on the surface of P[(*R*)-3HB] film takes place via two steps:[45] the first step is adsorption of enzyme on the surface of P[(*R*)-3HB] film via the binding domain, and the second step is hydrolysis of the polymer chain into water-soluble products by the catalytic domain.

The primary degradation products of P[(*R*)-3HB] chains by PHB depolymerases of *A. faecalis* and *P. pickettii* were monomer and dimer,[40] which may suggest preferential attack from the chain ends (*exo* attack). However, the rates of enzymatic erosion of P[(*R*,*S*)-3HB] stereoisomer films with isotactic diad fractions of 0.68–0.92 were higher than the rate of P[(*R*)-3HB] film, and trimer and tetramer were generated as degradation products with monomer and dimer, due to the presence of undegradable *S* units.[27,40] This result indicates that *endo* (random) cleavage of P(3HB) chain by the depolymerase occurs together with *exo* cleavage.[39]

Here, we propose a model of enzymatic hydrolysis of P(3HB) films by PHB depolymerase, which is illustrated in Figure 7. In this model, we suggest that the binding domain of depolymerase adheres selectively to the P[(*R*)-3HB] crystalline phase on the surface of P(3HB) film, and that the catalytic domain hydrolyzes predominantly P(3HB) chains in the amorphous phase on the surface and subsequently erodes P(3HB) chains in the crystalline phase. P(3HB) polymer chains in an amorphous phase are mobile at temperatures above T_g of around 4 °C, while P(3HB) polymer chains in a crystalline phase are rigid and have a 2_1 helix conformation.[57] The lamellar thickness of P[(*R*)-3HB] in a crystalline state are in the range of 6–10 nm. The PHB depolymerase may be liable to adhere to stable crystalline lamellae of P[(*R*)-3HB], while it may hardly bind to mobile P(3HB) chains in an amorphous state. Consequently, atactic P[(*R*,*S*)-3HB] components in the miscible blend films with P[(*R*)-3HB] may be degraded by PHB depolymerase in the presence of crystalline P[(*R*)-3HB]. On the other

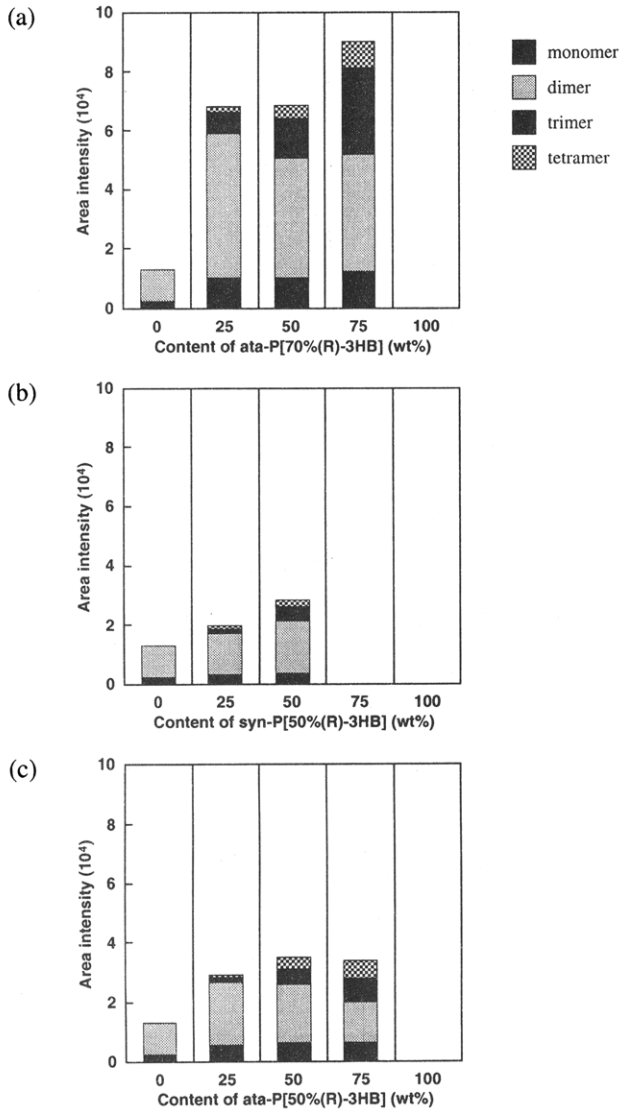

Figure 6. The composition and weight distributions of water-soluble products after enzymatic degradation of P[(*R*)-3HB]/P[(*R*,*S*)-3HB] blend films for 3 h at 37 °C in an aqueous solution (pH 7.4) containing PHB depolymerase (2.0 μg/mL) from *P. pickettii*: (a) P[(*R*)-3HB]/ata-P[70%(*R*)-3HB] blend, (b) P[(*R*)-3HB]/syn-P[50%(*R*)-3HB] blend, and (c) P[(*R*)-3HB]/ata-P[(*R*)-3HB] blend.

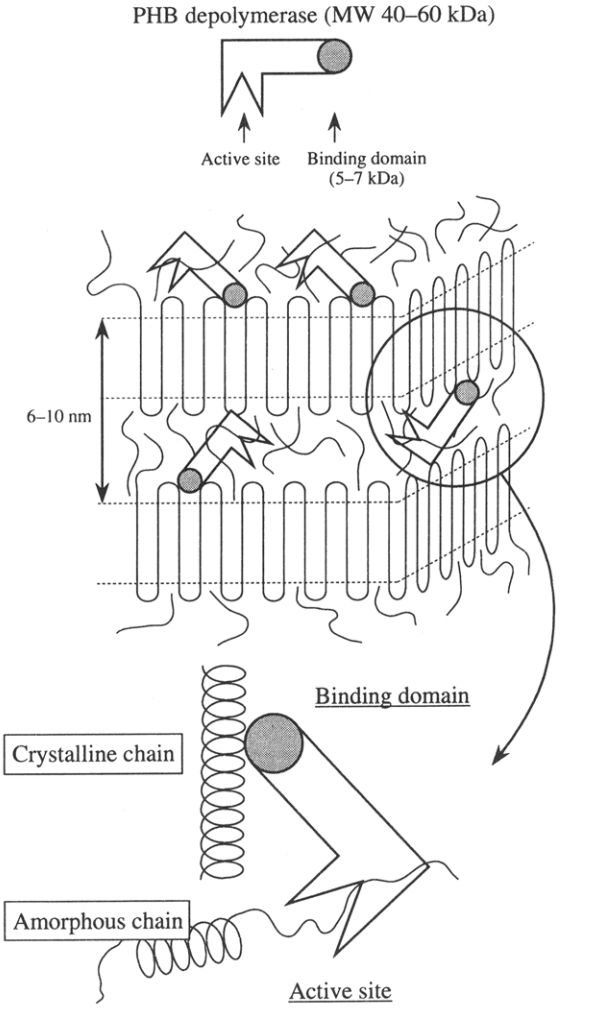

Figure 7. A model of enzymatic hydrolysis of P(3HB) chains by PHB depolymerase consisting of binding and catalytic domains.

hand, amorphous atactic P[(*R*,*S*)-3HB] polymers may be hardly eroded by PHB depolymerase, since PHB depolymerase hardly adsorbs on the surface of amorphous polymers. In this study, a low crystalline syndiotactic P[(*R*,*S*)-3HB] was also hardly hydrolyzed by PHB depolymerase. This result may be related to the presence of crystal defects within the lamellae core and in the crystalline–amorphous interface of a low-crystalline syndiotactic P[(*R*,*S*)-3HB]. The X-ray diffraction pattern of syndiotactic P[(*R*,*S*)-3HB] sample ([*i*] = 0.30) was broad, suggesting that crystal defects were located within crystalline lamellae.[40] It is likely that such crystal defects weaken the adsorption of PHB depolymerase to crystalline lamellae. In addition, the rate of enzymatic hydrolysis of P(3HB) chains depends on the molecular structure of 3HB monomer units. The enzyme is incapable of hydrolyzing the sequence of (*S*)-3HB units.[16,27] The concentrations of (*R*)-3HB unit on the surface of P[(*R*)-3HB]/ata-P[70%(*R*)-3HB] blend films are higher than those of other two types of P[(*R*)-3HB]/P[50%(*R*)-3HB] blend films. Therefore, the rates of enzymatic degradation of P[(*R*)-3HB]/ata-P[70%(*R*)-3HB] blend films were much faster than those of other two types of P[(*R*)-3HB]/P[50%(*R*)-3HB] blend films.

Acknowledgment. The authors thank Dr. Yoji Hori, Takasago International Corporation, for kindly supplying the samples of atactic P[70%(*R*)-3HB] and syndiotactic P[50%(*R*)-3HB].

References and Notes

(1) Doi, Y. *Microbial Polyesters*; VCH Publishers: New York, 1990.
(2) Anderson, A. J.; Dawes, E. A. *Macrobiol. Rev.* **1990**, *54*, 450.
(3) Marchessault, R. H.; Coulombe, S.; Morikawa, H.; Okamura, K.; Revol, J. F. *Can. J. Chem.* **1981**, *59*, 38.
(4) Barham, P. J.; Keller, A.; Otun, E. I.; Holmes, P. A. *J. Mater. Sci.* **1984**, *19*, 2781.
(5) King, P. P. *J. Chem. Tech. Biotecnol.* **1982**, *32*, 2.
(6) Chowdhury, A. A. *Arch. Microbiol.* **1963**, *47*, 167.
(7) Delafield, F. P.; Doudoroff, M.; Pallerroni, N. J.; Lusty, C. J.; Contopoulos, R. *J. Bacteriol.* **1965**, *90*, 1455.
(8) Tanio, T.; Fukui, T.; Shirakura, Y.; Saito, T.; Tomita, K.; Kaiho, T.; Masamune, S. *Eur. J. Biochem.* **1982**, *124*, 71.
(9) Jansen, P. H.; Harfoot, C. G. *Arch. Microbiol.* **1990**, *154*, 253.
(10) (a) Mergaert, J.; Anderson, C.; Wouters, A.; Swings, J.; Kersters, K. *FEMS Microbiol. Rev.* **1992**, *103*, 317. (b) Mergaert, J.; Webb, A.; Anderson, C.; Wouters, A.; Swings, J. *Appl. Environ. Microbiol.* **1993**, *59*, 3233.
(11) Jendrossek, D.; Knode, I.; Habibian, R. B.; Steinbüchel, A.; Schlegel, H. G. *J. Environ. Polym. Degrad.* **1993**, *1*, 53.
(12) Schirmer, A.; Jendrossek, D.; Schlegel, H. G. *Appl. Environ. Microbiol.* **1993**, *59*, 1220.
(13) Yamada, K.; Mukai, K.; Doi, Y. *Int. J. Biol. Macromol.* **1993**, *15*, 215.

(14) Mukai, K.; Yamada, K.; Doi, Y. *Polym. Degrad. Stab.* **1993**, *41*, 85.
(15) Mukai, K.; Yamada, K.; Doi, Y. *Polym. Degrad. Stab.* **1994**, *43*, 319.
(16) Lusty, C. J.; Doudoroff, M. *Proc. Natl. Acad. Sci. U.S.A.* **1966**, *56*, 960.
(17) Brucato, C. L.; Wong, S. S. *Arch. Biochem. Biophys.* **1991**, *290*, 497.
(18) Kumagai, Y.; Kanesawa, Y.; Doi, Y. *Makromol. Chem.* **1992**, *193*, 53.
(19) Agostini, D. E.; Lando, J. B.; Shelton, J. R. *J. Polym. Sci., Polym. Chem. Ed.* **1971**, *9*, 2775.
(20) Tani, H.; Yamashita, S.; Teranishi, K. *Polym. J.* **1972**, *3*, 417.
(21) Teranishi, K.; Iida, M.; Araki, T.; Yamashita, S.; Tani, H. *Macromolecules* **1974**, *7*, 421.
(22) Iida, M.; Araki, T.; Teranishi, K.; Tani, H. *Macromolecules* **1977**, *10*, 275.
(23) (a) Yasuda, T,; Aida, T.; Inoue, S. *Macromolecules* **1983**, *16*, 1792. (b) Yasuda, T.; Aida, T.; Inoue, S. *Macromolecules* **1984**, *17*, 2217.
(24) Billingham, N. C.; Proctor, M. G.; Smith, J. D. *J. Organomet. Chem.* **1988**, *341*, 83.
(25) Gross, R. A.; Zhang, Y.; Konrad, G.; Lenz, R. W. *Macromolecules* **1988**, *211*, 2657.
(26) Bloembergen, S.; Holden, D. A.; Bluhm, T. L.; Hamer, G. K.; Marchessault, R. H. *Macromolecules* **1989**, *22*, 1656.
(27) Doi, Y.; Kumagai, Y.; Tanahashi, N.; Mukai, K. *Biodegradable Polymers and Plastics*; Vert, M., et al. Eds.; Royal Society of Chemistry: London, 1992; p 139.
(28) Hocking, P. J.; Marchessault, R. H. *Polym. Bull.* **1993**, *30*, 163.
(29) Takeichi, T.; Hieda, Y.; Takayama, Y. *Polym. J.* **1988**, *20*, 159.
(30) Shelton, J. R.; Agostini, D. E.; Lando, J. B. *J. Polym. Sci., Polym. Chem. Ed.* **1971**, *9*, 2789.
(31) Zhang, Y.; Gross, R. A.; Lenz, R. W. *Macromolecules* **1990**, *23*, 3206.
(32) Le Borgne, A.; Spassky, N. *Polymer* **1989**, *30*, 2312.
(33) Tanahashi, N.; Doi, Y. *Macromolecules* **1991**, *24*, 5732.
(34) Kemnitzer, J. E.; McCarthy, S. P.; Gross, R. A. *Macromolecules* **1992**, *25*, 5927.
(35) (a) Kemnitzer, J. E.; McCarthy, S. P.; Gross, R. A. *Macromolecules* **1993**, *26*, 1221. (b) Kemnitzer, J. E.; McCarthy, S. P.; Gross, R. A. *Macromolecules* **1993**, *26*, 6143.
(36) Hori, Y.; Suzuki, M.; Yamaguchi, A.; Nishishita, T. *Macromolecules* **1993**, *26*, 5533.
(37) Kricheldorf, H. R.; Lee, S. R.; Scharnagl, N. *Macromolecules* **1994**, *27*, 3139.
(38) Jesudason, J. J.; Marchessault, R. H.; Saito, T. *J. Environ. Polym. Degrad.* **1993**, *1*, 89.
(39) Hocking, P. J.; Timmins, M. R.; Scherer, T. M.; Fuller, R. C.; Lenz, R. W.; Maechessault, R. H. *Macromol. Rapid Commun.* **1994**, *15*, 447.
(40) Abe, H.; Matsubara, I.; Doi, Y.; Hori, Y.; Yamaguchi, A. *Macromolecules* **1994**, *27*, 6018.
(41) Abe, H.; Doi, Y.; Satkowski, M. M.; Noda, I. *Macromolecules* **1994**, *27*, 50.
(42) Kumagai, Y.; Doi, Y. *Makromol. Chem., Rapid Commun.* **1992**, *13*, 179.
(43) Okawara, R.; Wada, M. *J. Organomet. Chem.* **1963**, *1*, 81.
(44) Doi, Y.; Tamaki, A.; Kunioka, M.; Soga, K. *Appl. Microbiol. Biotechnol.* **1988**, *28*, 330.
(45) Mukai, K.; Yamada, K.; Doi, Y. *Int. J. Biol. Macromol.* **1993**, *15*, 361.
(46) Grubisic, Z.; Rempp, R.; Benoit, H. *J. Polym. Sci., Part B* **1967**, *5*, 753.
(47) Vonk, C. G. *J. Appl. Crystallogr.* **1973**, *6*, 148.
(48) Hoffman, J. D.; Weeks, J. J. *J. Chem. Phys.* **1965**, *42*, 4301.
(49) Fukui, T.; Narikawa, T.; Miwa, K.; Shirakura, Y.; Saito, T.; Tomita, K. *Biochim. Biophys. Acta* **1988**, *952*, 164.
(50) Saito, T.; Suzuki, K.; Yamamoto, J.; Fukui, T.; Miwa, K.; Tomita, K.; Nakanishi, S.; Odani, S.; Suzuki, J.; Ishikawa, K. *J. Bacteriol.* **1989**, *171*, 184.
(51) Saito, T.; Iwata, A.; Watanabe, T. *J. Environ. Polym. Degrad.* **1993**, *1*, 99.
(52) Gilkes, N. R.; Henrissat, B.; Kilburn, D. G.; Miller, R. C.; Warren, R. A. J. *Microbiol. Rev.* **1991**, *55*, 303.
(53) Watanabe, T.; Suzuki, K.; Oyanagi, W.; Ohnishi, K.; Tanaka, H. *J. Biol. Chem.* **1990**, *265*, 15659.
(54) Robbins, P. W.; Overbye, K.; Albright, C.; Benfield, B.; Pero, J. *Gene* **1992**, *111*, 69.
(55) Wong, K. K. Y.; Tan, L. U. L.; Saddler, J. N. *Microbiol. Rev.* **1992**, *52*, 305.
(56) Briese, B. H.; Schmidt, B.; Jendrossek, D. *J. Environ. Polym. Degrad.* **1994**, *2*, 75.
(57) Cornibert, J.; Marchessault, R. H. *J. Mol. Biol.* **1972**, *71*, 735.

MA941190Z